International Journal of Advanced Research in Biological Sciences

ISSN : 2348-8069

www.ijarbs.com

Research Article

Structural, optical and dielectric properties of nanosized $Mg_{0.88}$ $Sr_{0.12}Fe_2O_4$ ferrite nanoparticles.

A.Loganathan[a*] and K.Kumar[b]

[a] Engineering Physics section, Annamalai University, Annamalai Nagar, Tamil Nadu, India -608 002,

[b] Department of Physics, Annamalai University, Annamalai Nagar, Tamil Nadu, India -608 002

*Corresponding author

Abstract

The present work deals with the structural, optical and dielectric properties of Sr ions substituted magnesium ferrite nanoparticles prepared by coprecipitation method by XRD (X-ray Diffraction), SEM (Scanning Electron Microscope), UV–vis DRS and dielectric measurement. Their structural and morphological character was investigated through XRD (X-ray Diffraction) and SEM (Scanning Electron Microscope). XRD result conform the formation of single phase spinel structured nanoferrite particles which crystalline size is 17nm. The substitution of Sr ions in the cubic ferrite lattice shows increased value of lattice constant. UV–vis DRS analysis was used to evaluate their optical property and band gap energy of ferrite particles. In order to identify their electrical transport mechanism, dielectric measurement was carried out at different temperature.

Keywords: Co-precipitation, UV-DRS, Dielectric propertie.

1.Introduction

In this modern era, Spinel ferrites system considered an excellent electronic material due to their special properties and used in High frequency devices, microwave devices, sensors, high quality filters, rod antennas, etc (Dixit et.al., 2012; Iqbal *et al*., 2013; Pradhan *et al*., 2005; Baruwati *et al*., 2007; Snelling, 1969). AB_2O_4 is the universal formula of spinel structure nanoparticles. Where, B is the trivalent (Fe^{3+})cation in octahedral positions and A is the divalent cation (Mg^{2+}, Cu^{2+}, Co^{2+}, Zn^{2+}, Mn^{2+}) located in tetrahedral positions of spinel structure. $MgFe_2O_4$ is a soft magnetic n-type semiconducting material which normally acquired in inverse spinel structure at room temperature, that is Mg^{2+} ions occupied in B-site and remaining Fe^{3+} ions occupied in A-site (Bamzai *et al*.,2013). The distribution of ions in the spinel structure strongly depends on synthesis process.

Several methods used for the preparation of ferrite nanoparticles, including combustion, sintering ceramic method, sol–gel, co-precipitation, combustion technique (Ming-Ru Syue *et al*.,2011; Mohammed *et al*.,2012; Sujatha *et al*.,2013; Rahman *et al*2013; Theophil Anand *et al*.,2015). Several reports available for the substitution of different metal ions in spinal structure and shows a considerable modification in their structural and electrical properties. A.C. Druc et.al report that substitution of Co ions in the magnesium ferrite materials increase in their dielectric loss (A.C. Druc *et al.*, 2014). M.A. El Hiti observed that the decreased value of tanδ while Mg^{2+} ions replaced by Zn^{2+} in $Mg_xZn_{1-x}Fe_2O_4$ ferrite system (Hiti,1999). Similarly, A. Manikandan et.al observed that the effect of Sr^{2+} ions in $Zn_{1-x}Sr_xFe_2O_4$ ferrite system and shows dramatic change in their structural, morphological and magnetic properties (Manikandan *et al*., 2013). M.A. Amer et.al noted that the structural and magnetic properties are mainly Sr^{2+} content depend (Amer *et al*.,2014). K.K. Bamzai et.al reported that the structural and morphological character of cubic phase $MgFe_2O_4$ modified with Dy ions (Bamzai *et al*., 2013). To the best of the author's knowledge, there is no such report on the effect of Sr^{2+} cation electrical properties of the $Mg_{0.88}Sr_{0.12}Fe_2O_4$ ferrite system.

2. Experimental procedure

Nanosized ferrite particles are prepared by conventional co-precipitation method. The starting chemicals used for preparation of ferrite particles were analytical grade. The initial aqueous solution was produced in distilled water by dissolving metal nitrates (iron nitrate, magnesium nitrate and strontium nitrate) according to desired stoichiometric proportion. The prepared solution was continuously stirred and headed on a magnetic stir up to one hour. Then the NaOH solution was mixed with metal nitrate solution as a precipitant at 90°C. The obtained precipitate was dried in electric oven at 100°C and calcinated for 3 hours in air atmosphere at 900°C. At the end, dried powder was mixed homogeneously in mortar and agate for 30 min to get the fine powder ferrite nanoparticles. The crystallite size, lattice constant, morphology, functional groups, optical and Dielectric properties were identified by using XRD, FT-IR, SEM,UV-DRS and dielectric studies.

3. Results and discussion

3.1 XRD analysis

Fig.1 depicted the XRD pattern of Sr^{2+} substituted $MgFe_2O_4$ nanoparticles calcinated at 900°C. From this spectrum, the diffraction pecks observed at 30°, 35.3°, 47°, 62 ° belongs to (220), (3 1 1), (4 0 0), (5 1 1), (4 4 0) plane respectively. The obtained peaks intensity and d-spacing values are readily indexed with pure magnesium ferrite nanoparticles (JCPDS file no.89-3084). The absences of other peaks indicate that synthesized nanoparticles are in single cubic phase. The crystalline size of calcinated $Mg_{0.88}Sr_{0.12}Fe_2O_4$ nanoparticles is theoretically estimated by Scherrer's formula in maximum intensity (311) plane using the following relation (Cullity, 1978).

$$D_{hkl}= K\lambda/\beta \cos \theta \quad (1)$$

Were, K is the shape factor, λ is the wave length of Cu Kα radiation, β is the full width at half maxima and θ is the Bragg's angle. The calculated crystalline size is 17nm. Further, the lattice constant also calculated by using d-spacing values obtained from XRD results.

$$a=d_{hkl}(h^2+k^2+l^2)^{1/2} \quad (2)$$

were, dhkl is the d-spacing values obtained in (311) plane and h,k,l are the miller indices, respectively. The calculated lattice constant value is 8.4381 Å. It is quite higher than literature values and JCPDS File no. of pure magnesium ferrite (Hankarea *et al*.,2009). This is due to large size Sr^{2+} (1.27Å) ions replaced by smaller Mg^{2+}(0.72Å) ions thus leads to expansion of unit cell volume.

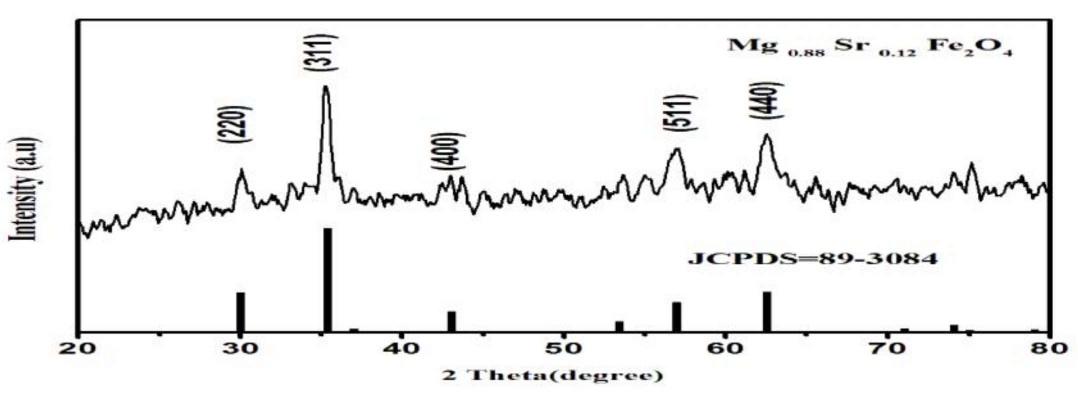

Fig.1. XRD spectrum of calcinated nanoparticles

3.2 Micro structural analysis

The microstructure of calcinated Sr substituted magnesium ferrite nanoparticles examined by the scanning electron microscopy technique and shown in Fig.2. From the figure, synthesized nanoferrite exhibits uniform distribution of grains with moderate agglomeration between grains. All the particles appear as a cluster. This may be due to magnetic interaction between synthesized particles (Rahman *et al*., 2013). From the deep observation in fig.2, some dark areas also observed due to presents of pores. The energy dispersive X-ray (EDX) spectrum of synthesized nanoparticles is shown in fig.2. EDX analysis conformed the existing of Mg, Sr, Fe and O element in prepared samples and obtained weight and atomic percentage of elements are listed in table (inset of Fig.2).

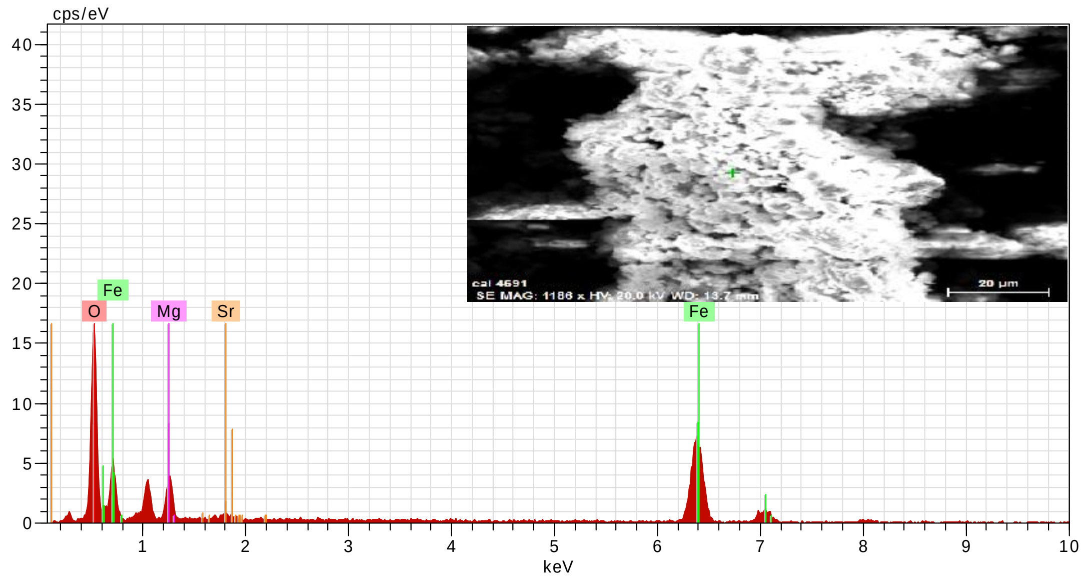

Fig.2. SEM image of Sr substituted Magnesium ferrite nanoparticles

The optical properties of Mg $_{0.88}$ Sr $_{0.12}$ Fe_2O_4 ferrite nanoparticles were studied by UV–vis DRS spectra recorded in the wavelength range between 200 and 1200 nm. Fig.3 depicts the room temperature UV–vis DRS spectra of the synthesized ferrite system which shows that the band-gap transition in visible region. The Kubelka–Munk function is used to convert the diffused reflectance (R) into equivalence absorption coefficient as given by following relation

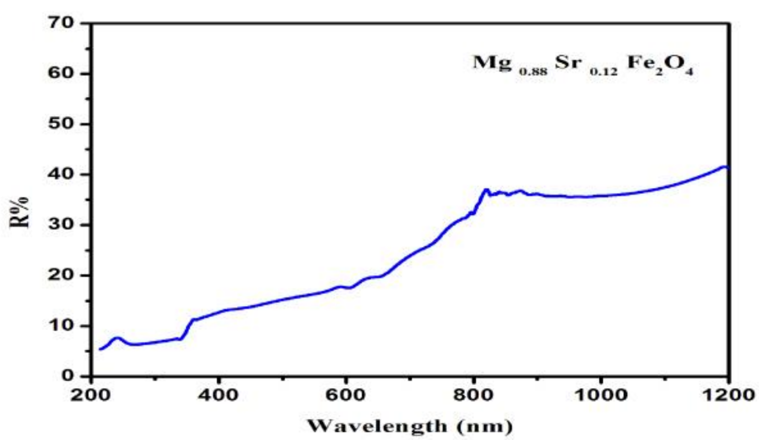

Figure.3. UV–vis diffuse reflectance spectra of nano-structure Sr substituted magnesium ferrite nanoparticles prepared by chemical co-precipitation method

$\alpha = F(R) = (1-R)^2/2R$ (3)

where F(R) is Kubelka–Munk function, α is the absorption co efficient, and R is the reflectance value. Furthermore, the absorption coefficient values are used to estimate the band gap energy of the present ferrite system by using Tauc relation.

$F(R)\, h\nu = A\,(h\nu - E_g)^2$ (4)

where h*v* is the photon energy. The band gap energy was estimated by plotting a graph between (αh*v*)2 versus photon energy (h*v*) as shown in fig.4. Extrapolation of linear regions of this plot gives the band gap energy of the present system. The estimated value of band gap energy of $Mg_{0.88}$ $Sr_{0.12}$ Fe_2O_4 ferrite nanoparticles is 2.8eV. Which is apparently blue shifted compared to reported values of pure Mg Fe_2O_4 system (2.0–2.2eV) (2.0–2.2eV) (Nipan *et al*., 2010; Kim *et al*., 2009). This may be due to the reduced particle size effect of nanoparticles (Manikandan *et al*., 2014).

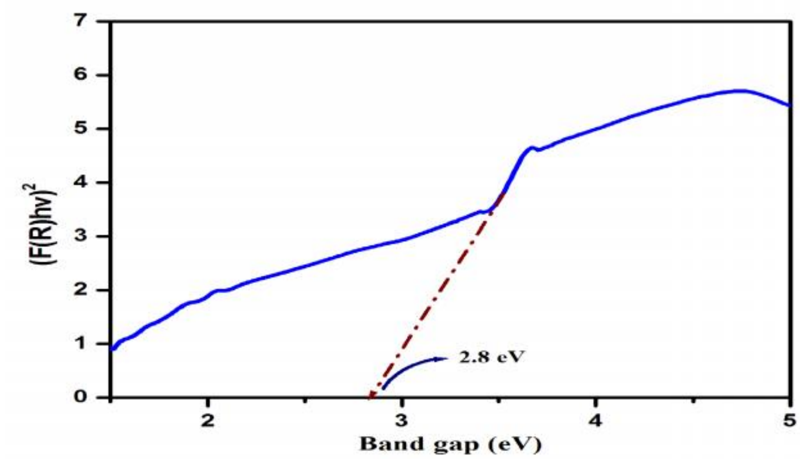

Figure.4. Plot of $(F(R)h\nu)^2$ vs. hν for band gap calculation of Sr substituted nanoparticles calcinated at 900^{o}C

3.4 Dielectric measurements

The dielectric behavior of nanoferrite system is an important property which is influenced by several factors such as preparation conditions, composition, ion distribution, calcination temperature, applied field strength, grain and grain boundary resistivity, etc. in the present work, the dielectric measurement was carried out in the temperature range of 30, 40, 60, 80 and 100^{o}C respectively. The real part and imaginary part of dielectric constants and ac conductivity (σ_{ac}) are calculated by following relations,

$\varepsilon' = Ct/\varepsilon_o A$ (5)

$\varepsilon'' = \varepsilon' \tan\delta$ (6)

$\sigma_{ac} = \varepsilon' \varepsilon_o \omega \tan\delta$ (7)

were t is the thickness of the pellet, A is the cross sectional area of the pellet, ε_{or} is the permittivity of free space, ω is an angular frequency (ω=2π*f*) and tanδ is the dielectric-loss. Fig. 4 and 5 shows the real part and imaginary part of the dielectric constant value observed at a different temperature range. In the present investigation, both real and imaginary part of the dielectric constant initially appeared as the maximum in the low frequency range and linearly decreases with the increase of frequency and is found to be attained constant in higher frequencies. It is the universal dielectric behavior of ferrite materials (Padmaraj *et al*.,2015; Maria Yousaf Lodhi *et al*., 2014). Maxwell–Wagner and Koops phenomenological theories were used to explain dielectric behavior of the present ferrite system. According to Maxwell–Wagner theory, the frequency dependent dielectric constant of present system explained on the basis of space charge polarization. The charge carriers produced by metal ions present in different valence state and contribute in the polarization process of ferrite materials.

At this low frequency range, charge carriers are align in the direction of the applied field and produce a high dielectric constant. But in high frequency range, they cannot orientate in applied field direction. This leads to decrease in dielectric constant at higher frequency ranges (Muhammad Azhar Khan *et al*., 2012). Koop's model suggested that the ferrite system contains two different parts of structure in the form of grain and grain boundary (Gul *et al*., 2008, Mangalaraja *et al*., 2002). The non-conducting grain boundary influenced at low frequency range and conducting grain influenced at higher frequency ranges. And all so, the dielectric constants were observed as the increasing trend with temperature. In investigating temperature range, the maximum dielectric constant is observed in the higher temperature range. The dielectric constant feebly increase in lower temperature ranges due to normally the charge carriers bounded with their lattice position and these temperatures not enough to make them free from their lattice. However, the dielectric constant effectively increased in higher temperature (100^{o}C) this may be due to sufficient energy supply to charge carriers free from their lattice position and they align themselves in the direction of the applied field.

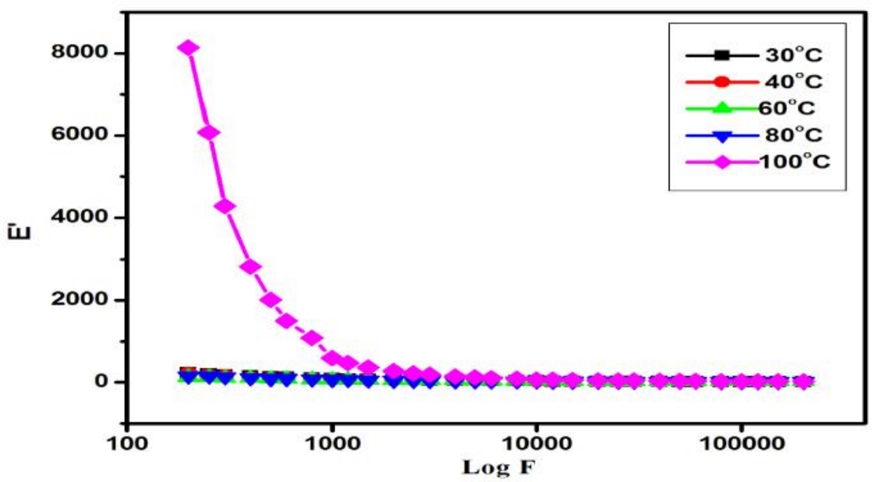

Figure.5 Variation of real part of dielectric constant as a function of frequency with different temperature

The ac conductivity of Mg $_{0.88}$ Sr $_{0.12}$Fe$_2$O$_4$ nanoferrite is shown in Fig.6. From the figure, the ac conductivity of ferrite system very feebly increases in lower frequency site and increased with increase in frequency. At the lower frequency range, the ac conductivity is due to presence of grain boundary contribution, whereas in higher frequency due to grain contribution. The ac conductivity slightly increases with temperature up to 90^{o}C after that which is immensely increased in 100^{o}C. It is due to the thermal activation of electrons (Varalaxmi and Sivakumar, 2014; Gabal *et al*., 2013).

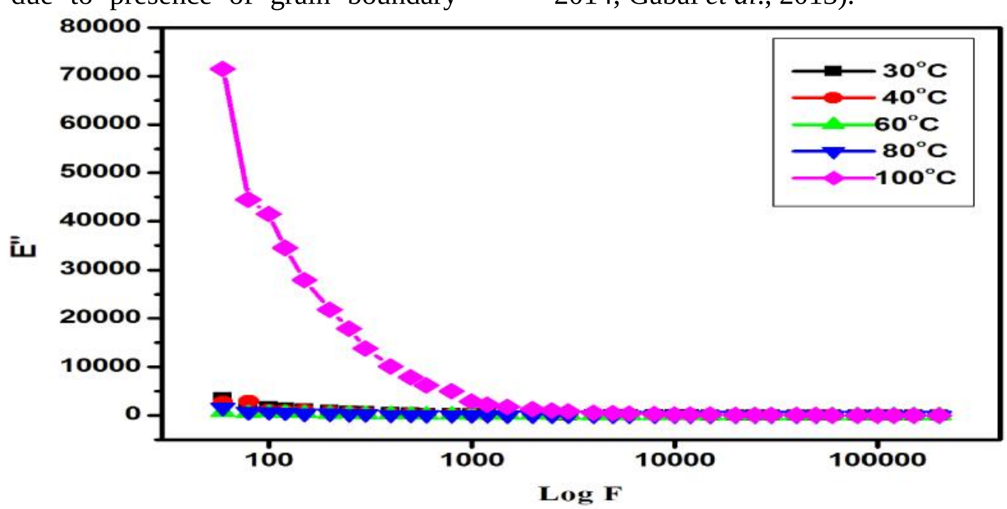

Figure.6 Variation of imaginary part of dielectric constant as a function of frequency with different temperature

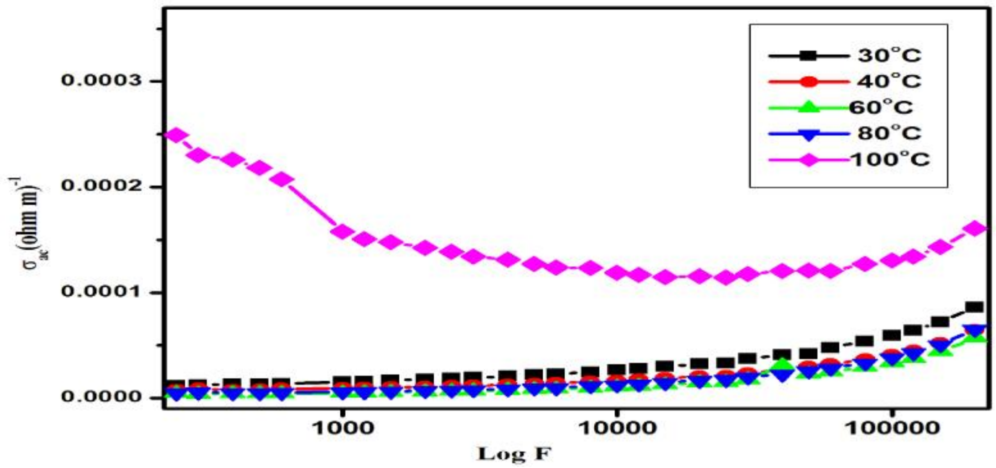

Figure.7 Variation of log σ_{ac} conductivity with frequency in different temperature

Conclusion

Nanosized Sr substituted $Mg_{0.88}$ $Sr_{0.12}Fe_2O_4$ ferrite particles prepared in co-precipitation method. The substitution of larger size ionic radii of Sr ions in magnesium ferrite leads to expansion of lattice constant. The XRD shows synthesized crystalline size is 17 nm and further SEM revealed that they are interacting with each other. The observed band gap value is approximately 2.8eV. Synthesized ferrite materials are shows universal dielectric behavior in investigating temperature and frequency range. Both the real and imaginary part of dielectric constant decrease with increase in frequency and temperature. CV characteristic shows the existence of pseudocapacitance process.

References

Amer M.A, Meaz T.M, Attalah S.S, Ghoneim A.I, Structural and magnetic characterization of the $Mg_{0.2-x}Sr_xMn_{0.8}Fe_2O_4$ nanoparticles, Journal of Magnetism and Magnetic Materials 363 (2014) 60–65.

Bamzai K.K, Gurbinder Kour, Kaur B, Kulkarni S.D, Effect of cation distribution on structural and magnetic properties of Dy substituted magnesium ferrite, Journal of Magnetism and Magnetic Materials 327 (2013) 159–166.

Bamzai K.K, Kour G, Kaur B, Kulkarni S.D, Effect of cation distribution on structural and magnetic properties of Dy substituted magnesium ferrite, Journal of Magnetism and Magnetic Materials 327 (2013) 159–166.

Baruwati B, Rana R.K, Manorama S.V, Further insights in the conductivity behavior of nanocrystalline NiFe2O4, J. Appl. Phys. 101 (2007) 014302.

Cullity B.D, Elements of X-ray-diffraction, second ed., Addison Wesley Publishing, Co., 89 (1978) 42–46.

Dixit G, Singh J.P, Srivastava R.C, Agrawal H.M, Magnetic resonance study of Ce and Gd doped NiFe2O4 nanoparticles, J.Magn.Magn.Mater. 324(2012) 479–483.

Druc A.C, Borhan A.I, Diaconu A, Iordan A.R, Nedelcu G.G, Leontie L, Palamaru M.N, How cobalt ions substitution changes the structure and dielectric properties of magnesium ferrite?, Ceramics International 40 (2014) 13573–13578.

Gabal M.A, Abdel-Daiem A.M, Al Angari Y.M, Ismail I.M, Influence of Al-substitution on structural, electrical and magnetic properties of Mn–Zn ferrites nanopowders prepared via the sol–gel auto-combustion method, Polyhedron 57 (2013) 105–111.

Gul I.H, Ahmed W, Maqsood A, J. Magn. Magn. Mater. 320 (2008) 270–275.

Hankarea P.P, Jadhav S.D, Sankpal U.B, Patil R.P, Sasikala R, Mulla I.S, Gas sensing properties of magnesium ferrite prepared by co-precipitation method, Journal of Alloys and Compounds 488 (2009) 270–272.

Hiti M.A, Dielectric behaviour in Mg-Zn ferrites, Journal of Magnetism and Magnetic Materials 192 (1999) 305-313.

Iqbal M.A, Islam M, Ashiq M.N, Ali I, Iftikhar A, Khan H.M, Effect of Gd substitiution on physical and magnetic properties of $Li_{1.2}Mg_{0.4}Gd_xFe_{(2-x)}O_4$ ferrites, J. AlloysCompd.579(2013)181–186.

Kim HG, Borse PH, Jang JS, Jeong ED, Jung OS, Suh YJ, Lee JS, (2009) Chem Commun 39:5889.

Mangalaraja R.V, Ananthakumar S, Manohar P, J. Magn. Magn. Mater. 253 (2002) 56.

Manikandan A, Judith Vijayaa J, John Kennedy L, Bououdina M, Microwave combustion synthesis, structural, optical and magnetic properties of $Zn_{1-x}Sr_xFe_2O_4$ nanoparticles, Ceramics International 39 (2013) 5909–5917.

Manikandan A, Sridhar R, Arul Antony S, Seeram Ramakrishna, A simple aloe vera plant-extracted microwave and conventional combustion synthesis: Morphological, optical, magnetic and catalytic properties of $CoFe_2O_4$ nanostructures, Journal of Molecular Structure 1076 (2014) 188–200.

Maria Yousaf Lodhi , Khalid Mahmood, Azhar Mahmood, Huma Malik, Muhammad Farooq Warsi, Imran Shakir, M. Asghar, Muhammad Azhar Khan, New $Mg_{0.5}Co_xZn_{0.5-x}Fe_2O_4$ nano-ferrites: Structural elucidation and electromagnetic behavior evaluation, Current Applied Physics 14 (2014) 716-720.

Ming-Ru Syue, Fu-Jin Wei, Chan-Shin Chou, Chao-Ming Fu,,Magnetic, dielectric, and complex impedance properties of nanocrystalline Mn–Zn ferrites prepared by novel combustion method, Thin Solid Films 519 (2011) 8303–8306.

Mohammed K.A, Al-Rawas A.D, Gismelseed A.M, Sellai A,Widatallah H.M, Yousif A, Elzain M.E, Shongwe M, Infrared and structural studies of $Mg_{1-x}Zn_xFe_2O_4$ ferrites, Physica B 407 (2012) 795–804.

Muhammad Azhar Khan, Islam M.U, Ishaque M, Rahman I.Z, Magnetic and dielectric behavior of terbium substituted $Mg_{1-x}Tb_xFe_2O_4$ ferrites, Journal of Alloys and Compounds 519 (2012) 156– 160.

Nipan GD, Ketsko VA, Stognij AI, Trukhanov AV, Koltsova TN, Kopeva MA, Elesina LV, Kuznetsov NT (2010) Inorg Mater 46:429.

Padmaraj O, Venkateswarlu M, Satyanarayana N, Structural, electrical and dielectric properties of spinel type $MgAl_2O_4$ nanocrystalline ceramic particles synthesized by the gel-combustion method, Ceramics International 41 (2015)3178-3185.

Pradhan S.K, Bid S, Gateshki M, Petkov V, Microstructure characterization and cation distribution of nanocrystalline magnesium ferrite prepared by ball milling, Materials Chemistry and Physics 93 (2005) 224–230.

Rahman S, Nadeem K, Anis-ur-Rehman M, Mumtaz M, Naeem S, Letofsky-Papst I, Structural and magnetic properties of Zn Mg-ferrite nanoparticles prepared using the co-precipitation method, Ceramics International 39 (2013) 5235–5239.

Snelling E.C, Soft Ferrites: Properties and Applications, first ed., Iliffe Books Ltd., London, 1969.

Sujatha Ch, Venugopal Reddy K, Sowri Babu K, Rama Chandra Reddy A, Buchi Suresh M, Rao K.H, Effect of Mg substitution on electromagnetic properties of NiCuZn ferrite, Journal of Magnetism and Magnetic Materials 340(2013)38–45.

Theophil Anand G, John Kennedy L, Judith Vijaya J, Kaviyarasan K, Sukumar M, Structural, optical and magnetic characterization of $Zn_{1-x}Ni_xAl_2O_4$ spinel nanostructures synthesized by microwave combustion technique, Ceramics International 41(2015)603–615.

Varalaxmi N, Sivakumar K.V, Structural and dielectric studies of magnesium substituted NiCuZn ferrites for microinductor applications, Materials Science and Engineering B 184 (2014) 88–97.